NJC

New Journal of Chemistry

A journal for new directions in chemistry

Accepted Manuscript

This article can be cited before page numbers have been issued, to do this please use: P. Dutta, S. Kumari, J. Jhonpeter, R. Sharma, G. vijaykumar, H. S. Das, S. P, S. Sil, S. K. Mandal, A. Sengupta and A. Sarkar, *New J. Chem.*, 2021, DOI: 10.1039/D0NJ06229D.

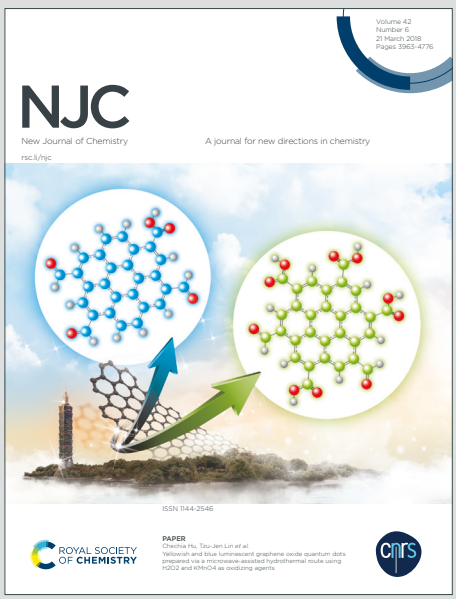

View Article Online
DOI: 10.1039/D0NJ06229D

Phenalenyl Based Platinum Anticancer Compounds with Superior Efficacy: Design, Synthesis, Characterization, and Interaction with Nuclear DNA

Pradip Dutta[a], Smita Kumari[a], Justin Paulraj[a] , Rupali Sharma[a], Gonela Vijaykumar[b], Hari Sankar Das[b], Sreejyothi P.[b], Swagata Sil[b], Swadhin K. Mandal[b], Aniruddha Sengupta[a]*, Arindam Sarkar[a]*

[a] India Innovation Research Center
465 Patparganj Industrial Area, Delhi 110092.
*Email: sararindam@gmail.com, anirudd.sengupta@gmail.com
[b] Department of Chemical Sciences, Indian Institute of Science Education and Research (IISER)-Kolkata, Mohanpur -741252, India.

Abstract: Significant efforts have been made to develop new platinum anticancer compounds since the discovery of cis-platin, however, non-specific toxicity or loss of efficacy remain some of the major challenges in this area of Platinum drug discovery. Newly developed platinum compounds, structurally distinct from the current molecules, imparting efficacy at lower concentrations than the current drugs, and interacting with DNA leading to cell death, may prove beneficial. In the current study, we designed, synthesized, and characterized three phenalenyl based platinum chloride compounds (**1**, **2,** and **3**) with the goal that labile Pt-Cl bond with a planar structure of phenalenyl moiety would enhance their interaction with DNA, leading to improved efficacy. In addition, it is assumed that the fluorescent property of these compounds would facilitate the mechanistic investigation. The crystal structure of compound **1** demonstrates a perfectly planar structure with a single Pt-Cl bond. *In-vitro* cell viability studies on cancer cell lines, including lung, colorectal, breast, and osteosarcoma revealed superior efficacy for compounds **1** and **2**, relative to platinum drugs in clinical use. Localization studies utilized the strong fluorescence of compound **3** to investigate the mechanism of action, revealing its interaction with DNA, leading to cell death. This study enriches the arsenal of potential platinum-based anti-cancer therapeutics and provides an easy-to-use tool for the mechanism of action studies of these compounds.

Keywords: Phenalenyl, Platinum, Fluorescence, Anticancer, Efficacious, DNA-binding

View Article Online
DOI: 10.1039/D0NJ06229D

Introduction:

Numerous metal complexes, demonstrating anticancer properties, have been designed and synthesized in past decades.[1-3] Among them, platinum drugs, such as cisplatin, carboplatin, and oxaliplatin are effective anticancer agents in clinical use against many solid tumors, either alone or in combination with other therapeutic compounds[4-6]. Approximately 10-20 % of all cancer patients are prescribed these platinum chemotherapeutic drugs, according to the United States' National Cancer Institute (NCI) database[7]. Since its discovery, cisplatin remains the most efficacious among them. Several Pt compounds have been synthesized in the last few decades but only a few of them demonstrated better efficacy than cisplatin[8,9]. Some of the Pt compounds showed similar or improved *in vitro* efficacy than cisplatin but were lacking a conventional mechanism of action which includes nuclear localization as well as compound DNA interaction[10-12]. Considering the current drug development practices; it would be a cumbersome process to develop a Pt drug that works through non-conventional mechanistic pathways. Pt compounds with enhanced efficacy and retaining the conventional mechanism of interaction with DNA to achieve cell killing would reduce the time for development and should be continually evaluated. Some of the structurally different Pt complexes, which interact with DNA, and are evaluated in clinical trials include satraplatin, polyplatinum compounds, and picoplatin[13].

The success of cisplatin as an anti-tumor drug is seen as a prototypical success story, leading to the development of subsequent platinum-based drugs, which emerged as standard chemotherapy for solid tumours[14,15]. The cross-linking of platinum drugs with DNA resulted in blockage of replication, inducing cell-cycle arrest and ultimately cell death, thus proving effective in various cancers[16,17]. This garnered interest in metal-DNA binding, with Pt-chemistry providing the platform for exciting bioinorganic chemistry research. Interestingly, similar coordination complexes with other metals have not been as successful. The mechanistic findings have thus prompted chemists to synthesize new anti-cancer Pt compounds, imparting efficacy through efficient interaction with DNA. Furthermore, the generation of cells/tumors resistant to platinum drugs has necessitated structures of these new molecules to be distinct from cisplatin and its derivatives. Besides, using the inherent fluorescence of an anticancer compound itself would be an added advantage to understand its mechanism of action[18,19]. Thus, an anticancer compound with Pt-Cl centre, combined with a fluorescent planar backbone, could be highly efficacious and is expected to follow the above-mentioned mechanistic path which can be easily realized by *in vitro* localization studies due to its inherent fluorescence. Phenalenyl based compounds have been widely used as molecular conductors[20], catalysts[21,22], and chemosensors[23,24]. More recent work from our group has used Phenalenone moiety in a pro-drug with similar active moiety and efficacy as that of

View Article Online
DOI: 10.1039/D0NJ06229D

Oxaliplatin[25]; but a novel drug candidate with phenalenyl framework has rarely been realized. Easily achievable hetero atom substitution in phenalenyl moiety can be useful for stable six-membered ring coordination with platinum and its emissive property might be useful for mechanistic investigations.

The above-mentioned cancer drug discovery challenges were taken into account while designing two Pt-chloride complexes (**1**, **2**) where a planar fluorescent active phenalenyl (PLY) framework is directly linked with Pt-Cl moiety and another compound (**3**) where Pt-Cl moiety is linked to phenalenyl framework through a linker; with the goals: i) labile Pt-Cl bond may contribute to efficacy, ii) planar backbone could enhance the efficacy due to intercalation/interaction with DNA, and iii) inherent fluorescence of PLY moiety would help to understand the mechanism of action.

The design principles of all the molecules discussed in this work are summarized in **Figure 1**. Compounds **1** and **2** are expected to have a perfectly planar backbone and a Pt(II) center with a labile Pt-Cl bond. Compound **3** though not perfectly planar, retains a planar phenalenyl moiety. In the current work, we have synthesized the three aforementioned compounds and characterized them. The single-crystal X-ray structure of compound **1** was analyzed in detail, and *in vitro* efficacy has been studied for all three compounds. Emission intensities of the compounds were compared. Due to the relatively stronger fluorescence of compound **3,** it was used to examine nuclear localization and compound-DNA interaction.

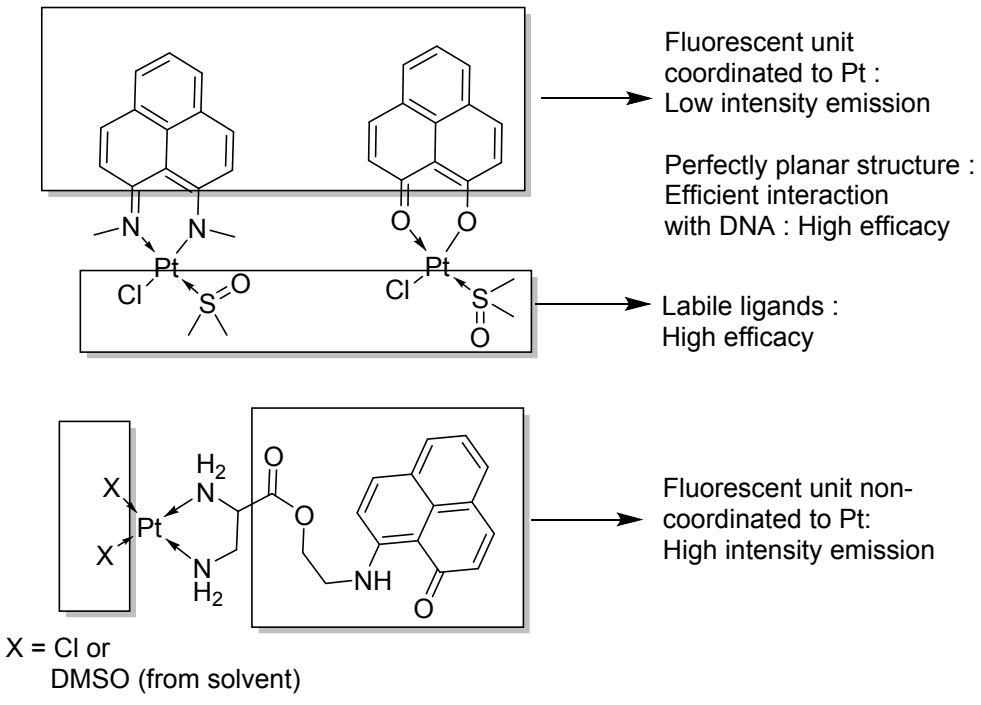

Figure 1. Design principles of molecules **1**, **2,** and **3**.

View Article Online
DOI: 10.1039/D0NJ06229D

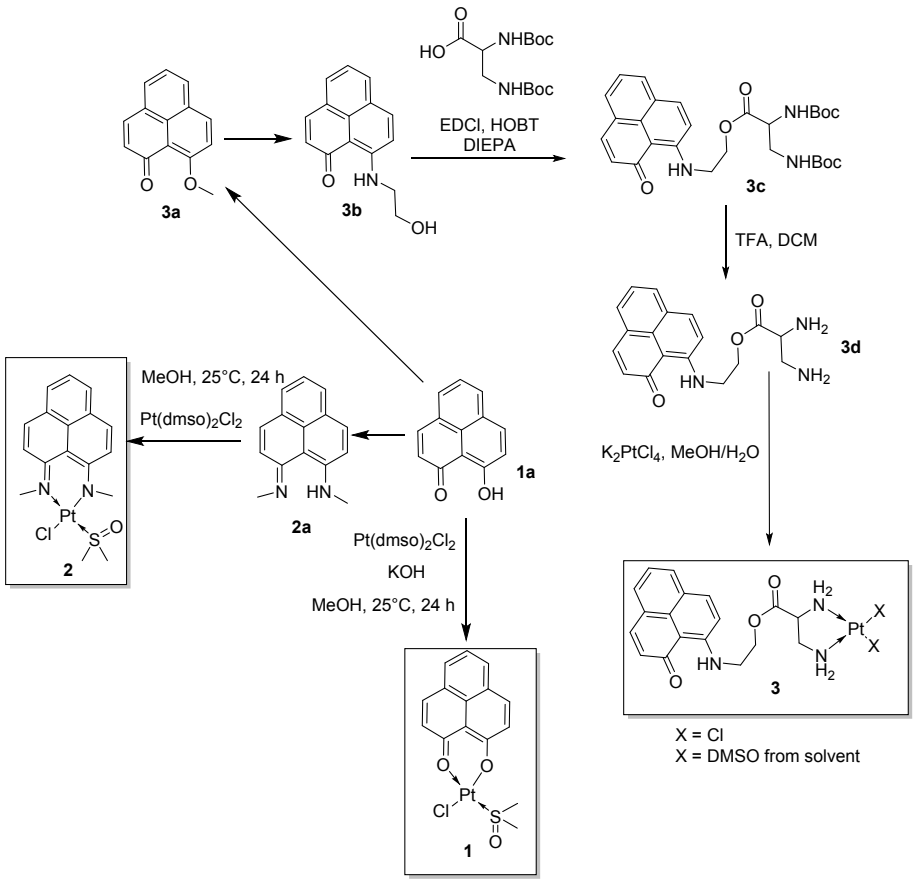

Scheme 1. Synthetic routes for molecules **1**, **2,** and **3.**

Results and discussion:

Synthesis and characterization of compounds 1, 2, and 3.

Compounds **1**, **2,** and **3** were synthesized starting from 9-hydroxyphenalenone (**1a**) (**Scheme 1**), a derivative of phenalenone which is a natural product obtained from plant extract[26]. Compound **1** was formed by reacting **1a** with $Pt(DMSO)_2Cl_2$ in presence of a base at RT whereas compound **2** was synthesized using a similar procedure but in absence of a base. In compounds **1** and **2**, one of the charges on the Pt atom was neutralized by the deprotonated phenalenyl ligand. Facile (without base) deprotonation of **2a** was realized by the stabilization of the conjugate base through delocalization over the PLY unit. The presence of a Dimethyl sulfoxide (DMSO) molecule in both **1** and **2** indicated by the presence of CH_3 peaks in ^1H NMR (**Figure S1a** and **S1b**) and molecular ion peak including a DMSO molecule in the ESI MS. Single-crystal X-ray structure of **1** confirmed the presence of one DMSO molecule which remained coordinated to Pt through the sulfur atom. Distinct doublets appeared in the ^1H NMR spectrum for all seven protons of phenalenyl unit,

View Article Online
DOI: 10.1039/D0NJ06229D

supporting the asymmetric structure of the molecules. The sharp peak in ^{195}Pt NMR spectrum at -2293 and -2729 ppm (**Figure S1d**, **S1e**), observed for **1** and **2**, established the fact that Pt is O,O, and N,N coordinated in these compounds, respectively. Compound **3** was synthesized from the diamino ligand **3d** which has been produced by a multistep procedure starting from **1a**. Compound **3a** was synthesized following the literature-reported procedure (see experimental). Successive reactions of amino alcohol followed by reaction of Boc protected diamines and deprotection by trifluoroacetic acid (TFA) resulted in the production of **3d**. Finally, the reaction of **3d** with K_2PtCl_4 produced the desired Pt chloride compound **3**. A single peak at -3255 ppm (**Figure S1f**) in the Pt NMR spectrum confirmed the diamino coordination to Pt. ^{1}H (**Figure S1c**) and ^{13}C NMR spectra also support the formation of compound **3**. Mass spectrum of compound **3** (**Figure S14**) in DMSO demonstrated the replacement of chemically labile chlorides with DMSO molecules. Pt-NMR chemical shift demonstrated a clear idea about the coordination environment of **1**, **2,** and **3**. Chemical shifts could be directly correlated with the coordinated atoms to the Pt center[27]. Two highly electronegative oxygen atoms are coordinated to Pt in **1** resulting in the Pt resonance occurring in a more deshielded region (-2293 ppm) than **2** and **3**. Compounds **2** and **3** are both coordinated to two N atoms, but the Pt in compound **3** is more shielded because it is coordinated to two sulfur (less electronegative than Chloride which is coordinated to Pt in **1** and **2**) atoms of DMSO molecules. Therefore, mass and NMR evidence support the replacement of chloride with DMSO molecules in **3**. This could be the reason for the higher IC_{50} of compound **3** as described in the later section of this manuscript. Thus, the structural features of all three compounds are predominated by Pt-Cl and Pt-DMSO bonding. Liang and co-workers have reported two Pt anticancer compounds which show one chloride and one DMSO coordination to Pt[28]. Recently, it has been shown that some monofunctional platinum complexes with only one site for binding with DNA have greater or similar efficacy than cisplatin[29-32]. Hence, we propose that the current series of compounds with a mono chloro Pt center (particularly compounds **1** and **2**) may be highly efficacious through their interaction with DNA.

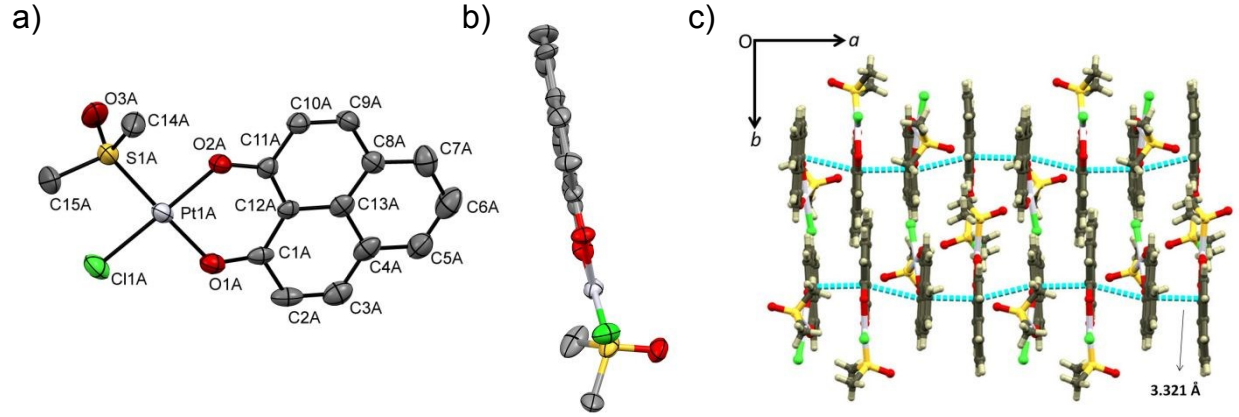

View Article Online
DOI: 10.1039/D0NJ06229D

Figure 2. Single crystal X-ray structure of compound **1** with a thermal ellipsoid plot drawn at 50% probability level; a) View perpendicular to PLY plane; b) View parallel to PLY plane, c) Molecular packing viewed along c axis-showing the 1-D network formed via $\pi--\pi$ interactions.

Table 1: Bond lengths and bond angles around Pt center, in the single-crystal X-ray structure of compound **1**.

Selected bonds and angles	Bond Lengths and angles
Pt1A-O1A	1.991(6) Å
Pt1A-O2A	2.012(6) Å
Pt1A-Cl1A	2.291(3) Å
Pt1A-S1A	2.184(3) Å
O2A-Pt1A-Cl1A	176.9(6)°
O1A-Pt1A-S1A	176.0(2)°

Crystallization and crystal structure analysis of compound 1:

Crystallization of compound **1** was performed in a chloroform/ether solvent mixture. It crystallized as dark brown colored single crystals in an orthorhombic system in a space group P21 21 21 with two molecules in the asymmetric unit. **Figures 2a** and **2b** show the orientation of a single molecule of **1**, perpendicular, and along the plane of the PLY unit respectively. **Figure 1a** indicates a nearly square planar coordination to the Pt center which is bonded to one S, two O, and one Cl atoms. Square planar orientation is also confirmed by the bond angles around Pt (**Table 1**). **Figure 2b** illustrates that phenalenyl unit is in the same plane as the Pt square plane. Thus, molecule **1** adopted a perfectly planar structure, suitable for intercalation among the grooves of the DNA helix. Pt-Cl bond length (2.29 Å, **Table 1**) in compound **1** is lower than the same bond lengths obtained in cisplatin (2.32 Å)[33]. This can be explained with a weaker trans effect of oxygen atoms of **1** than that of the nitrogen atoms in cisplatin. Due to the unavailability of the crystal structure, we could not compare the Pt-Cl bond lengths of compound **2** with **1** or cis-platin. In the crystal packing, the molecules are packed to form a one-dimensional network via π-π interactions between neighboring phenalenyl planes shown in **Figure 2c** displaying an interplanar distance between the phenalenyl planes as 3.321 Å.

Emission spectra of compounds 1, 2, and 3: In a recent publication[23], we demonstrated the factors affecting the fluorescence intensity of phenalenone framework. Interference from the non-conjugated electrons of the substituted hetero atoms deactivates fluorescence through inter-combinational conversions. In the current work, direct coordination of PLY to Pt may result in charge transfer phenomena between metal and ligand which is observed in many Pt complexes[34,35]. Charge transfer between PLY and Pt may deactivate the intra-ligand fluorescence of PLY moiety of **1** and **2**, resulting in low emission intensity of these compounds. In compound **3**,

View Article Online
DOI: 10.1039/D0NJ06229D

PLY is not directly coordinated to Pt, thus the emission intensity, resulting from PLY moiety, of this compound is expected to be higher than **1** and **2**. **Figure S17** describes the emission spectra of the three compounds.

Biological activities of compounds and intracellular localization studies:

Clinically approved platinum drugs have been extensively studied across various cancers using the National Cancer Institute's 60-cell-line panel[36,37]. A549 (non-small cell lung adenocarcinoma), HCT116 (colorectal carcinoma), T47D (mammary ductal carcinoma), U2OS (osteosarcoma), and MCF7 (breast adenocarcinoma) cell lines were selected to evaluate the cytotoxic ability of the three molecules synthesized in this study (compounds **1**, **2** and **3**). The cytotoxic effects of these compounds were compared to clinically approved platinum drugs at platinum equivalent concentrations ranging from 0-50 μM. The IC_{50} values for the compounds tested are tabulated in **Table 2**. Results of the MTT assay indicate low IC_{50} values observed for compounds **1** and **2**, relative to comparative platinum drugs in the tested cell lines, indicating their improved efficacy. In addition to lung, colorectal, and breast cancer, where platinates are used clinically, compounds **1** and **2** also show superior efficacy as monotherapy in osteosarcoma. These observations substantiate our hypothesis that compounds with a mono-chloro Pt center and a perfectly planar structure have superior efficacy. Morphology of A549 cells following 24 h treatment with 10 μM of compounds show rounded cells, ready to detach from plates treated with compounds **1** or **2**, while those treated with **3** had altered cell morphology, but were still adherent to the plates (**Figure S18**). This suggests a higher efficacy for compounds **1** and **2** in comparison to **3**, thus the imaging data corroborates the IC_{50} values recorded for the compounds.

Table 2: Comparative IC_{50} (μM) of compounds **1**, **2**, **3,** and marketed platinum drugs across human cancer cell lines.

	IC_{50} value (μM)					
Cell line	**Compound 1**	**Compound2**	**Compound 3**	**Oxaliplatin**	**Carboplatin**	**Cisplatin**
A549	2.73 ± 0.38	2.86 ± 0.70	23.58 ± 1.97	8.08 ± 1.18	>50	6.74 ± 1.28
HCT116	1.02 ± 0.36	1.01 ± 0.18	21.48 ± 4.02	2.92 ± 0.44	>50	7.76 ± 0.82
T47D	0.77 ± 0.69	1.71 ± 0.35	30.17 ± 8.01	9.53 ± 2.61	>50	9.28 ± 3.60
U2OS	0.73 ± 0.21	2.57 ± 1.13	35.77 ± 5.86	2.80 ± 0.61	>50	3.56 ± 0.95
MCF7	2.82 ± 0.24	2.5 ± 0.41	>50	27.6 ± 6.66	>50	11.62 ± 2.41

The structure of molecules synthesized suggested that the emitted fluorescence intensity would be higher for **3**, in comparison to **1** and **2** and intracellular localization studies corroborated the same (**Figure S19**). Recordable fluorescence intensity for microscopic imaging was observed only

for compound **3**, hence it was selected for subsequent *in vitro* imaging studies. We tried exploring the cellular localization of all the compounds; however, as depicted in **Figure S17**, emission intensities of **1** and **2** are 20 times lower than that of **3**, hence they could not be utilized for monitoring cellular localization. We incubated cells with a higher concentration of compounds **1** and **2**, with the hope of getting some recordable fluorescence intensity. However, due to the low IC_{50} values for both compounds, either the A549 cells rounded up and detached from the surface or cell death was observed. Due to relatively lower efficacy and higher emission intensity, compound **3** was ideal for the internalization/mechanistic studies. Intracellular localization of compounds **3** and **1a** was examined in A549 cells. The compounds were dissolved in organic solvents (DMSO or DMA) and cells were treated with molar equivalent concentrations. Image of cells was recorded under a fluorescent microscope; 18-20 hours post-treatment.

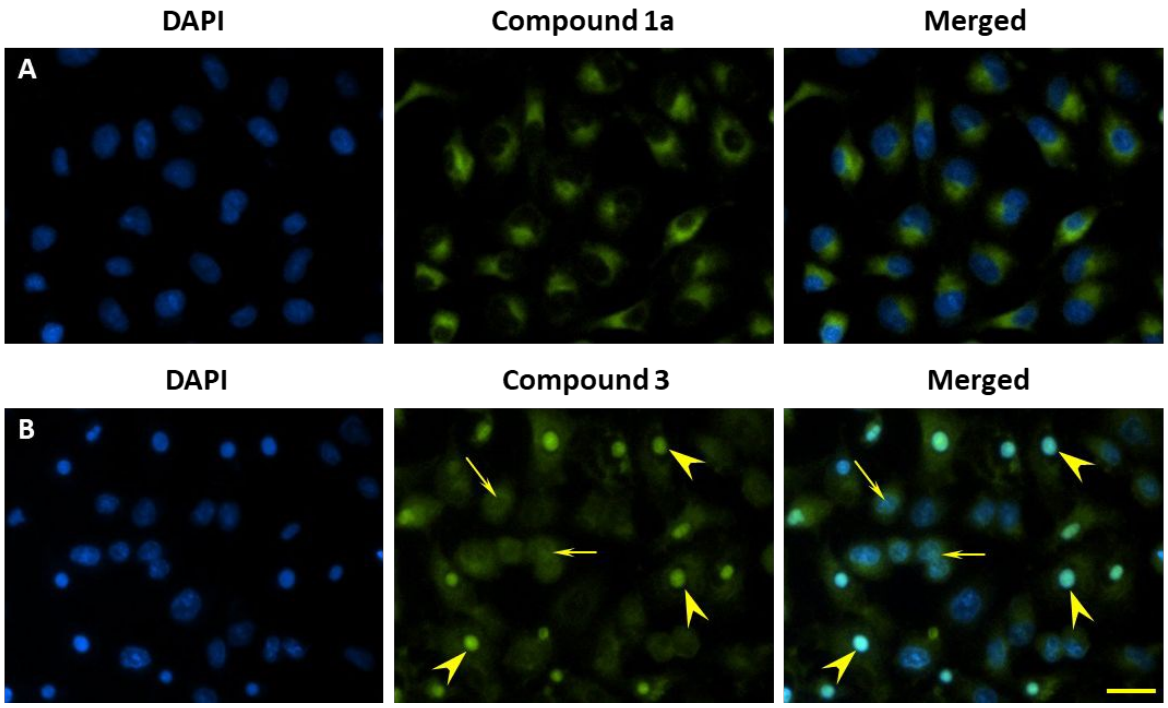

Figure 3. Intracellular localization of (**A**) Compound **1a** and (**B**) Compound **3** in A549 cells. Nuclear condensation assessment of cells by DAPI staining. Scale bar 20 μm.

Samples treated with compound **1a** had intense fluorescence in the cytoplasm, with almost no staining observed in the nucleus (**Figure 3A**), while cells treated with compound **3** show fluorescence throughout the cell (**Figure 3B**). A diffused green fluorescence was noted in both the nucleus and cytoplasm of treated cells (arrow). Additionally, an intense fluorescence was observed in nuclei (arrowhead) of few cells treated with compound **3**, which had condensed nuclei,

View Article Online
DOI: 10.1039/D0NJ06229D

as depicted through 4′,6-diamidino-2-phenylindole (DAPI) staining, which was supported by higher magnification images of the nuclei (**Figure S20)**.

The nuclear condensation phenomenon is a result of chromatin modulation and is observed for many DNA-binding compounds, including cisplatin[38,39]. We speculated that this nuclear condensation, observed only in cells treated with compound **3**, could designate cells destined for cell death. To examine if the treated cells conformed to these properties, A549 cells were subjected to treatment with compound **3**, following which, one set of unfixed cells was stained with DAPI, while the other was stained with propidium iodide (PI). Our results indicate that PI co-localizes with condensed nuclei in cells treated with compound **3** (**Figure 4**). PI is a fluorescent DNA-binding dye, which can penetrate cell membranes of dead or dying cells but is excluded from viable cells[40]. Therefore, our observations suggest that cells with condensed nuclei have compromised cell membrane and are directed towards death as a result of compound treatment.

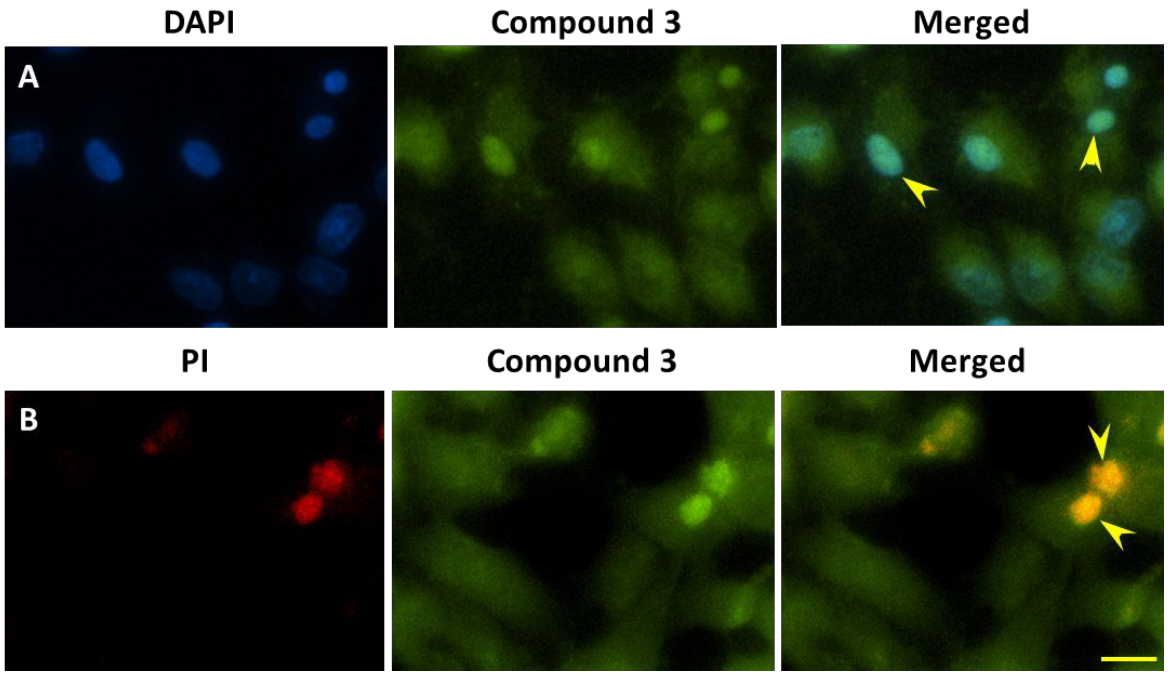

Figure 4. Staining of A549 cells with (**A**) DAPI and (**B**) PI show overlapping of Compound **3** fluorescence in cells with condensed nuclei (arrowhead). Scale bar 20 μm.

View Article Online
DOI: 10.1039/D0NJ06229D

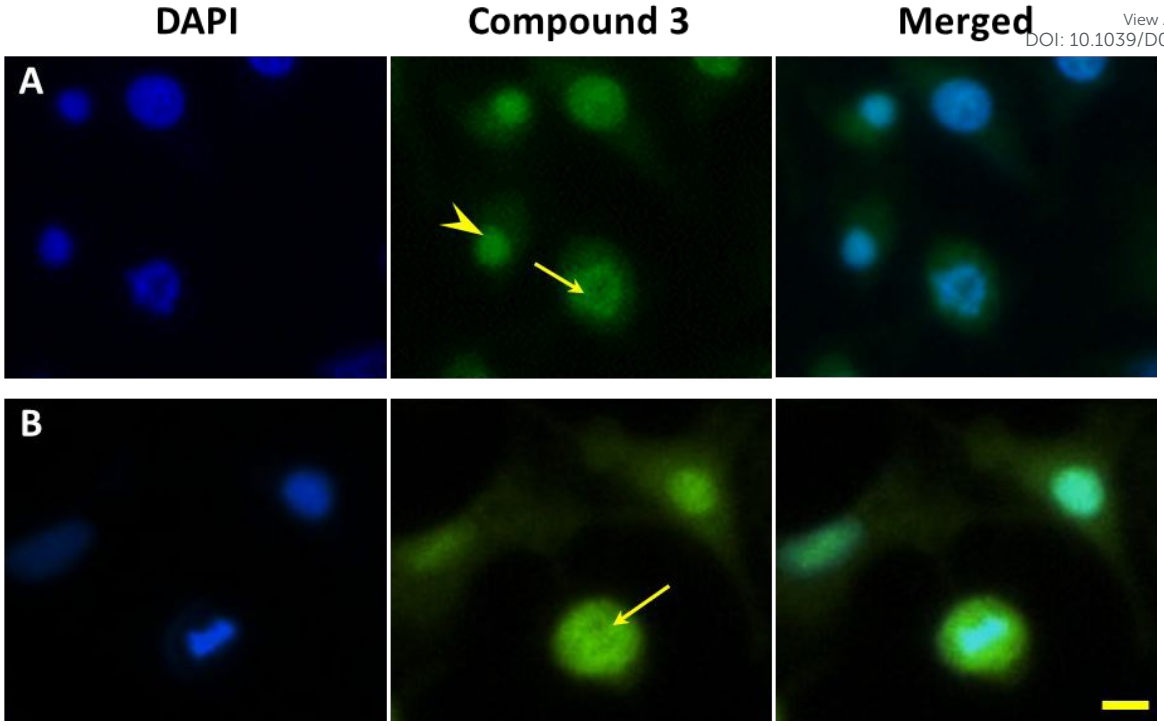

Figure 5. Fluorescence from Compound **3** in the condensed nucleus (arrowhead), (**A**) pro-metaphase, and (**B**) and metaphase chromosome (arrows) of A549 cells. Scale bar 10 μm.

Compound **3** was generated with the goal of trying to understand the mechanism of action for this class of compounds. Employing the intracellular fluorescence of this molecule, we wanted to evaluate if it could interact with DNA. Cellular localization studies reveal that fluorescence from compound **3** not only localizes with condensed nucleus (arrowhead); but also, completely overlays with DAPI staining of DNA (arrow) in pro-metaphase (**A**) or metaphase (**B**) chromosome (**Figure 5**). This observation clearly substantiates the interaction of the compound with DNA, also corroborating the retention of PLY moiety during the interaction.

Stability and reactivity study of compound 1:

Chloride is the only labile ligand in all three compounds (**1**, **2,** and **3**). Thus we have chosen compound **1** as the representative example to understand the stability in physiological conditions. Time-dependent ^{1}H NMR spectra in **Figure S21** show that the compound is stable in PBS (pH 7.4) up to 12 h. The reaction of Pt anticancer compounds with 5'-GMP has been considered as a standard experimental procedure to understand their reactivity with DNA nucleo-bases. [41, 42] Thus an NMR experiment was performed with compound **1** and 5'-GMP (Guanosine-5'-monophosphate) (1:2 mole ratio) in deuterated methanol/chloroform. The result is shown in **Figure S22**. Shift in H8 (of 5'-GMP) resonance indicates that the N7 is reacting/interacting with **1**. The appearance of new peaks after 2 h indicates the formation of a new compound in the solution. Significant reduction of stability of **1** in presence of 5'-GMP is the key feature of these two NMR

View Article Online
DOI: 10.1039/D0NJ06229D

experiments. Mass spec (**Figure S23**) of the reaction mixture confirms the formation of the 5'-GMP adduct with compound **1**.

Experimental section:

General methods: All reagents were procured from Sigma or Spectrochem and were used without further purification unless otherwise stated. All reactions were carried out with dried and freshly distilled solvents under an anhydrous atmosphere. K_2PtCl_4 was purchased from Arora Matthey. 5'-GMP was purchased from Sigma as the sodium salt. For melting point determination, the Buchi B-540 melting point apparatus was used. ^{1}H, ^{13}C, ^{195}Pt NMR spectra were recorded in Bruker Avance III 500 MHz or JEOL 400 MHz spectrometer. ^{195}Pt NMR was recorded with K_2PtCl_4 as an external reference (dissolved in D_2O and the reference value was set at -1616 ppm). HRMS was obtained by the Agilent QTof instrument. Compounds **1a**[43], **2a**[44], **3a**[45] were synthesized following literature procedures. Mass and NMR spectra of compounds **1**, **2**, **3,** and their intermediates are shown in **Figure S1** to **S15**. For the purity determination of compound **3**, analytical HPLC was carried out using a Waters e2695 system with a PDA (2998) detector inline. Reprosil C18 (250 mm x 4.6 mm, 5 µm; Dr. Maisch, Germany) column was used as stationary phase for the experiment with 5% acetonitrile-water gradient system; injection vol 60 ul; run time 40 min.

Synthesis and characterization of Compound 1: Compound **1a**, 0.090 g, 0.47 mmol) was placed in 250 mL single necked, round bottom flask and dissolved in 100 mL methanol. After that $Pt(DMSO)_2Cl_2$ (compound **b**, 0.2 g, 0.47 mmol) was added to the reaction medium. Subsequently, KOH (26.6 mg, 0.47 mmol) in 1 mL methanol was added. The reaction mixture was stirred for 18 hours in a nitrogen atmosphere at room temperature. The reaction was terminated once a yellowish precipitate was formed. The precipitate was filtered using ordinary filter paper and dried over a vacuum. The compound was purified by crystallization from a chloroform/diethyl ether solvent mixture. Yield (0.08 g, 35%). m.p. 133-134 °C;

Anal. Cal. (For $C_{15}H_{13}ClO_3PtS$) C, 35.76; H, 2.60; Found: C, 34.97; H, 2.86; ESIMS (m/z) calcd for $C_{15}H_{13}ClO_3PtS$ $(M+K)^+$, 542.95, found 542.9; ^{1}H NMR (400 MHz, $CDCl_3$, δ, ppm) : 8.13-8.17 (t, *J* = 8 Hz, 3 H), 8.09 (d, *J* = 8 Hz, 1 H), 7.62 (t, *J* = 8 Hz, *J* = 4 Hz, 1 H), 7.46 (d, *J* = 8 Hz, 1 H), 7.34 (d, *J* = 8 Hz, 1 H), 3.59 (s, 6 H). ^{13}C NMR (125 MHz, $CDCl_3$, δ, ppm): 172.31, 172.25, 139.85, 139.17, 132.72, 132.62, 126.86, 126.37, 126.22, 125.73, 124.46, 113.88, 44.25. ^{195}Pt NMR (107 MHz, DMSO-d6, δ, ppm): -2293.25.

Synthesis and characterization of compound 2: Compound **2a** (0.105 g, 0.47 mmol) was placed in a 250 mL single necked, round bottom flask and dissolved in 100 mL methanol. After that, Pt $(DMSO)_2Cl_2$ (0.2 g, 0.47 mmol) was added to the reaction medium. The reaction mixture was stirred for 18 hours in a nitrogen atmosphere at room temperature. The reaction was

View Article Online
DOI: 10.1039/D0NJ06229D

terminated once the purple precipitate was formed. The precipitate was filtered and dried over a vacuum. Yield (0.076g, 30%). m.p. 131-133 °C.

Anal. Cal. (For $C_{17}H_{19}ClN_2OPtS$) C, 38.53; H, 3.61; N, 5.29; Found: C, 38.19; H, 3.44; N, 5.39. ESIMS m/z calcd for $C_{17}H_{20}N_2OPtS$ $[M + H]^+$, 530.06, found 530.03;^{1}H NMR (400 MHz, $CDCl_3$,δ, ppm) : 7.75 (d, *J* = 8 Hz, 2H), 7.67 (d, *J* = 8 Hz, 1H), 7.60 (d, *J* = 8 Hz, 1H), 7.19-7.27 (m, 3H), 3.79 (s, 3H), 3.55 (s, 3H), 3.35 (s, 6H). ^{13}C NMR (125 MHz, $CDCl_3$, δ, ppm): 153.94, 153.80, 135.16, 134.71, 130.23, 130.14, 128.13, 125.66, 125.46, 121.68, 118.0, 117.81, 114.19, 47.83, 44.93, 43.69. ^{195}Pt NMR (107 MHz, DMSO-d6, δ, ppm) : -2729.08.

Synthesis and characterization of compound 3:

Synthesis of 3b: 9-Methoxy phenalenone **3a** (250 mg, 1.189 mmol) was placed in a pressure tube and dissolved in 2 mL dichloromethane. After that 3 mL of ethanolamine was added to the reaction mixture. It was refluxed for 18 h and the reaction was terminated once compound formation was observed. The crude product was purified by column chromatography using silica gel 60-120 mesh and MeOH:$CHCl_3$ (1:99) to obtain 100 mg (Yield 35%) of compound **3b**.

ESIMS m/z Calcd for $C_{15}H_{13}NO_2$, $[M]^+$, 239.09, found 239.97; ^{1}H NMR (400 MHz, DMSO-d_6, δ, ppm) 12.20 (s, 1 H), 8.19 (d, *J* = 4 Hz, 1 H), 8.06 (d, *J* = 4Hz, 1 H), 8.0 (t, *J*= 8Hz ,*J*= 8Hz, 2 H), 7.46-7.50 (m,2 H), 6.85 (d, *J*= 8 Hz, 1 H), 5.03 (t, *J*= 4Hz ,*J*= 4Hz, 1H) , 3.70-3.75 (m,2H), 3.65-3.70 (m, 2H); ^{13}C NMR (125 MHz, DMSO-d_6, δ, ppm) δ: 183.44, 156.25, 138.78, 138.83, 132.15, 131.89, 128.85, 128.14,124.74, 124.32, 122.14, 115.69, 107.54, 60.35, 45.30.

Synthesis of HOCOCH(NHBoc)CH_2CH(NHBoc):

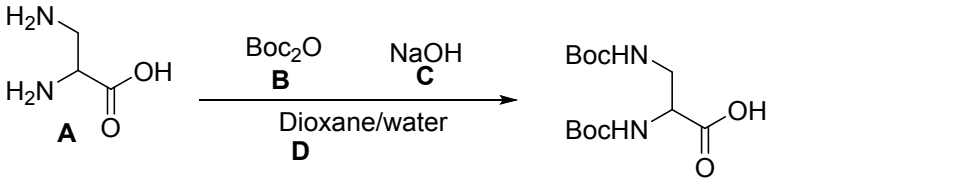

HOCOCH(NHBoc)CH2CH(NHBoc)

Compound **A** (1 g, 9.60 mmol) was placed in a 50 mL single-necked, round bottom flask and dissolved in 20 mL dioxane. After that, a solution of sodium hydroxide **C** (1.53 g, 38.4 mmol, in 15 mL water) was added. The reaction mixture was stirred at RT for 15 min. Boc anhydride **B** (5.23g, 24 mmol) was introduced and the stirring was continued for 12 h. Reaction completion was confirmed by TLC. To terminate the reaction, the reaction mixture was acidified using NaH_2SO_4 and extracted using ethyl acetate (3X20 mL). The organic layer was dried over sodium sulfate and concentrated under vacuum to get 900 mg of crude product.

Synthesis of 3c: Boc protected 2,3-diaminopropionic acid (38mg,1 eq) was placed in a 50 mL single necked, round bottom flask with 2.5 eq (60 mg) of EDCl and 1.5 eq (17 mg) of HOBt in dry dichloromethane and stirred at 0°C in an ice bath for 1h under nitrogen atmosphere. To this cooled

solution, compound **3b** (30 mg,1 eq) and DIEPA (64µL, 3eq) were added and the reaction was stirred overnight. After termination of the reaction, the crude product was purified by column chromatography (Silica 60-120 mesh, 2% MeOH/DCM) to obtain 50 mg (yield 76%) of **3c**.

ESIMS m/z calcd for $C_{28}H_{26}O_5N_3$, $[M+Na]^+$, 548.23, found 548.23 and 325.36 $[M+H\text{-}Boc]^+$; ^{1}H NMR (400 MHz, DMSO-d_6, δ, ppm) 12.26 (s, 1 H), 8.05 (d, *J* = 8 Hz, 1 H), 7.89-7.94 (q, 3H), 7.48 (t, *J*= 8Hz ,*J*= 4Hz, 1 H), 7.26 (d, *J*= 8 Hz, 1 H), 7.12 (d, *J*= 4 Hz, 1 H), 5.99 (s, 1H) , 5.76 (s, 1H), 4.62 (s, 1H) , 4.43 (s, 2H) , 3.89 (bs,2H), 3.61 (bs, 2H), 1.38 (s, 9H), 1.27 (s,9H); ^{13}C NMR (125 MHz, DMSO-d_6, δ, ppm): 184.40, 174.69, 170.76, 156.19, 138.98, 138.64, 132.15, 131.71, 128.72, 128.11, 127.65, 125.17, 124.45, 122.10, 113.97, 108.40, 79.99, 79.55, 63.39, 60.42, 54.91, 42.24, 41.19, 29.70, 21.06, 20.72, 14.20, 14.08.

Synthesis of 3d: Deprotection of Boc group was carried out by the addition of 30% TFA in dichloromethane (5 mL) to 50 mg of compound **3c**. TFA was removed under reduced pressure and the compound dissolved again in DCM and ether. This process was repeated twice and the crude product **3d** was used for the next step.

ESIMS m/z calcd. for $C_{17}H_{19}O_3N_3$ $[M+H]^+$, 326.14, found, 326.06; ^{1}H NMR (400 MHz, DMSO-d_6, ppm) δ**:** 12.19-12.23 (m, 1 H) ,8.26 (d, *J* = 8 Hz, 1 H), 8.10 (d, *J* = 8Hz, 1 H), 8.04 (t, *J*= 8Hz , *J*= 4Hz, 2 H), 7.50-7.56 (m,2 H), 6.88 (d, *J*= 4 Hz, 1 H), 6.55(s,1H), 4.50 (t, *J*= 4Hz , *J*= 4Hz, 2 H), 4.36 (t, *J*= 4Hz , *J*= 8Hz, 1 H) , 3.92-4.06 (m,3H), 3.36-3.40 (m, 2H) , 3.26-3.31 (m, 2H); ^{13}C NMR (125 MHz, DMSO-d_6, δ, ppm) : 184.40, 174.69, 170.76, 156.19, 138.98, 138.64, 132.15, 131.71, 128.72, 128.11, 127.65, 125.17, 124.45, 122.10, 113.97, 108.40, 79.99, 79.55, 63.39, 60.42, 54.91, 42.24, 41.19, 29.70, 21.06, 20.72, 14.20, 14.08.

Synthesis of compound 3: Compound **3d** (obtained from 50 mg of **3c**) in water was placed in a 50 mL single necked round bottom flask. After that aqueous solution of K_2PtCl_4 (9mg, 1eq) was added dropwise. Following the reaction, immediate precipitation was observed. The reaction mixture was stirred overnight and then lyophilized the next day to remove water. The crude mixture obtained was washed with water, methanol, and dichloromethane to get 20 mg crude product. Further purification was carried out by precipitation from DMF/Water to obtain 10 mg (yield 18%) of compound **3**. The purity of the compound was found to be 87% by HPLC (**Figure S16**).

ESIMS m/z calcd for $C_{17}H_{19}O_3N_3PtCl_2$, 590.04, found, 556.07 $[M\text{-}Cl\text{-}H]^+$, 713.11[M-2Cl+2DMSO] (compound was solubilized in DMSO for Mass); ^{1}H NMR (400 MHz, DMSO-d_6, ppm) δ**:** 12.18-12.24 (m, 1 H) ,8.22-8.28 (m,1H), 8.07-8.12 (m,1 H), 8.00-8.06 (m,2H), 7.49-7.55 (m,2 H), 6.87 (d, *J*= 8Hz, 1 H), 5.30-6.65(m, 4H) , 4.34-4.56 (m,2 H), 3.87-4.02 (m, 2H) 3.68-3.82 (m,1H), 2.88-3.03 (m,1H), 3.70-3.80 (m,1H); ^{13}C NMR (125 MHz, DMSO-d_6, ppm) δ: 183.17,155.44, 138.42, 138.11, 131.66, 131.41, 128.00, 127.25, 124.13, 123.71, 121.67, 114.63, 106.99, 64.22, 60.10, 59.93, 48.35, 47.98; ^{195}P NMR (100 MHz, DMSO-*d*6, δ, ppm) **:** -3247.70.

View Article Online
DOI: 10.1039/D0NJ06229D

Fluorescence measurement of complexes

Fluorescence measurements were carried out using a FluoroMax-4 spectrofluorometer from HORIBA Jobin Yvon, at a $2x10^{-5}$ M concentration of metal complexes in MeOH.

Single-crystal X-ray crystallography

A suitable crystal was selected and intensity data were collected on a Bruker D8 Venture diffractometer. The crystal was kept at 293(2) K during data collection. Using Olex2[46], the structure was solved with the Superflip[47,48,49] structure solution program using Charge Flipping and refined with the ShelXL[50] refinement package using Least Squares minimization.

Cell lines and reagents: The human cancer lines used in this study included A549 (non-small cell lung adenocarcinoma), HCT116 (colorectal carcinoma), T47D (mammary ductal carcinoma), U2OS (osteosarcoma), and MCF7 (breast adenocarcinoma). The cells were grown in 10 cm^2 plates or 25 cm^2 flasks, containing Dulbecco's Modified Eagle Medium (DMEM), (HiMedia), supplemented with 10% fetal bovine serum (FBS), 100 units/ml penicillin, and 100 µM streptomycin in a fully humidified incubator at 37°C in an atmosphere containing 5% CO_2 and 95% air. Cells were grown to 75-80% confluency, washed with phosphate-buffered saline (PBS), and harvested using 1X Trypsin-EDTA (HiMedia) for cell passaging. Clinical grade platinum drugs (cisplatin, carboplatin, and oxaliplatin) were used for comparative studies and were freshly diluted in culture media before usage.

Cytotoxicity assay: Cells were grown in culture plates/flasks, counted and adjusted to required concentrations and seeded in quadruplicate in 96-well plates, and allowed to attach overnight at 37°C in a humidified incubator with 5% CO_2. The compounds were freshly dissolved in DMSO and filtered through a 0.2 µm syringe filter. Cells were treated with compounds **1**, **2,** and **3** or cisplatin, carboplatin, and oxaliplatin (0-50 µM dose) and grown for 72 h. All subsequent dilutions from the stock were made in cell culture media.

Cell survival was assessed by colorimetric MTT assay, where 20 µLof 5 mg/mL MTT (HiMedia) solution was added to the media, and cells were incubated for another 2 h. The media containing MTT was completely removed and formazan precipitate was dissolved using 100 µLof 1:1 solution of DMSO:methanol. Wells containing DMSO:methnaol alone was recorded as blank to measure the background. The absorbance of plates was recorded in a microplate reader (iMark, BioRad) at 550 nm, with background correction at 655 nm.

Untreated cells were used as the control for all subsequent calculations. The absorbance for untreated cells was considered 100% viability. Cell survival and dose-response in cell lines erewere plotted using the GraphPad PRISM software (GraphPad). The IC_{50} values were

calculated from the resultant graphs and results tabulated as mean ± SEM, from at least three independent experiments.

Nuclear staining of cells: A549 cells were seeded on clean coverslips to 60% confluency. The cells were then treated for 18-20 h with 50 μM platinum equivalent concentration of **3** and **1a**, diluted in DMEM. Fixation of cells was carried out using 4% paraformaldehyde for 5 min, followed by permeabilization with 0.5% Triton X-100 in PBS and washing thrice with PBS. Cells were counterstained with 1 μg/ml DAPI solution for 2-3 min, washed thrice with PBS, and coverslips were inverted and mount with prolong anti-fade mounting media (Molecular Probes) onto microscope slides.

Unfixed cells were treated with 1 μg/mL DAPI solution or PI in PBS for 5 min and 10 min, respectively. The cells on coverslips were washed once with PBS and fixed with 4% paraformaldehyde for 5 min. Following fixation, cells were washed thrice with PBS, the coverslips were inverted and mount with prolong anti-fade mounting media (Molecular Probes) onto microscope slides. Imaging was carried out using an epifluorescence microscope (Nikon TiE epifluorescence microscope).

Stability Check for Compound 1

$8x10^{-3}$ mmol of compound **1** was dissolved in 500 ul DMSO-d6 in an NMR tube and the 1H NMR spectra were recorded. To this, 200 ul PBS (pH 7.4) was added and ^{1}H NMR spectra were recorded in 0h, 2h, 6h, and 12h time intervals.

Reactivity check for Compound 1 with 5'-GMP

In another experiment $8x10^{-3}$ mmol compound **1** was dissolved in Methanol-d4/Chloroform-d mixture. To this $16x10^{-3}$ mmol 5'-GMP was added and ^{1}H NMR spectra were recorded in 0h, 2h, 6h, 24h, and 48h time intervals. NMR solution was submitted for mass analysis after 48h.

Conclusion:

In the current study, we have synthesized and characterized three Pt compounds (**1**, **2,** and **3**), with a planar structure having fluorescent active phenalenyl moieties. Detailed structural and spectral characterization of the compounds revealed that **3** is highly fluorescent whereas **1** and **2** were weakly emissive due to their differences in coordination with Pt. Compounds **1** and **2** exhibited superior efficacy than marketed platinum drugs, under *in vitro* cytotoxicity studies in human cancer lines. Inherent fluorescence of compound **3** helped in carrying out cellular localization studies, which reveals that this class of compound accumulates in the nucleus and interacts with DNA.

Platinum compounds are often used to study drug-DNA crosslinking and chromosomal integrity using sophisticated techniques[51,52]. In this study, we report a DNA-interacting fluorescent molecule, which can be a tool to study Metallo-pharmaceutical mechanisms. Furthermore, the improved efficacy of these compounds warrants *in vivo* research into various cancer models. Combinatorial therapy may be the way forward in our fight against cancer and we hope the

reported compounds, with their low IC_{50} values in combination with other drugs, differing in modes of action would offer a wide range of effective therapeutic options.

Author Contributions

Dr. Pradip Dutta: Synthesis and characterization of compounds 1 and 2, Data Curation, Formal analysis, Manuscript review, Resource organization, Investigation

Smita Kumari: Performed all biology experiments, Biology Experiment Validation, Formal analysis, Investigation

Dr. Justin Paulraj: Synthesis and characterization of compound 3

Rupali Sharma: Chemistry data validation, Manuscript review and editing, Resource organization

Dr. Gonela Vijaykumar: Resolve single-crystal X-ray structure, Writing-review of crystallographic section.

Dr. Hari Sankar Das: Conducted emission experiments of all compounds.

Dr. Sreejyothi P: Conducted stability experiment, Data curation

Dr. Swagata Sil: Conducted GMP experiment

Dr. Swadhin Mandal: Conceptualization, Resource organization, Funding acquisition

Dr. Aniruddha Sengupta: Supervision of biology work, Manuscript original draft biology part writing-review and editing, Fund acquisition, Formal analysis

Dr. Arindam Sarkar: Conceptualization, Supervision of chemistry and analytical work, Funding acquisition, Project administration, Investigation, Manuscript Original Draft writing

Conflicts of Interest

There are no conflicts to declare

Acknowledgments

The work was supported by the Science and Engineering Research Board (SERB), Government of India (Grant No. EMR/2016/000357).

Electronic Supplementary Information

Supporting information for this article contains NMR and mass spectra of complexes and intermediates; Emission plots of complexes; crystals data table etc. CCDC 2049882 contains the supplementary crystallographic data of compound **1** for this paper.

References

1. N. J. Farrer, L. Salassa and P. J. Sadler, *Dalton Trans*., 2009,**235**,10690-10701.
2. P. C. A. Bruijnincx and P. J. Sadler, Curr. Opin. *Chem. Biol*., 2008, **12**, 197-206.
3. C. G. Hartinger, N. M. Nolte and Paul J. Dyson, *Organometallics,* 2012, **31**, 5677–5685.
4. M. Galanski, M. A. Jakupec and B. K. Keppler, *Curr Med Chem*. 2005, **12**, 2075-94.
5. N.A. Yusoh, H. Ahmad and M.R. Gill, *Chem Med Chem*. 2020, **15**, 2121-2135.
6. J.N. Bodor, V. Kasireddy and H. Borghaei, *J Oncol Pract.* ,2018,**14**,529–35.
7. (https://www.cancer.gov/research/progress/discovery/cisplatin).
8. T.C. Johnstone, K. Suntharalingam and S. J. Lippard, *Chem. Rev*., 2016, **116**, 3436-3486.
9. L. Kelland, *Nat. Rev. Cancer* ,2007, **7**, 573–584.
10. Z.J. Wang, H. Renata, N.E. Peck, C.C. Farwell, P.S. Coelho and F.H. Arnold, *Angew Chem.* 2014, **126**, 6870–6874.
11. K. Mitra, S. Gautam, P. Kondaiah and A.R. Chakravarty, *Angew. Chem. Int. Ed*. 2015, **54**, 13989–13993.
12. K.L. Ciesienski, L.M. Hyman, D.T. Yang, K.L. Haas, M.G. Dickens, R.J. Holbrook and K.J. Franz, *Eur. J. Inorg. Chem*., 2010, 2224– 2228.
13. K. S. Lovejoy and S. J. Lippard, *Dalton Trans*., 2009, 10651–10659.
14. D. Wang and S.J. Lippard, *Nat Rev Drug Discov.,* 2005 Apr, **4**, 307-320.
15. Y Jung and S.J. Lippard, *Chem Rev.* 2007 May,**107,** 1387-1407.
16. F.M. Muggia, A. Bonetti, J.D. Hoeschele, M. Rozencweig and S.B. Howell, *Oncogene*, 2003, **22**, 7265–7279.
17. F.M. Muggia, A. Bonetti, J.D. Hoeschele, M. Rozencweig and S.B. Howell, *J Clin Oncol*, 2015 Dec10, **33**, 4219-26.
18. Z. Chen, S. Zhang, L. Shen, Z. Zhu and J. Zhang, *New J. Chem*., 2015, **39**, 1592-1596.
19. E. Wong and C. M. Giandomenico, *Chem. Rev*., 1999, **99**, 2451-2466.
20. S. K. Pal, M. E. Itkis, F. S. Tham, R. W. Reed, R. T. Oakley and R. C. Haddon, *Science,* 2005, **309**, 281–284.
21. A. Mukherjee, T. K. Sen, P. K. Ghorai and S. K. Mandal, *Organometallics* ,2013, **32**, 7213–7224.
22. A. Pariyar, G. Vijaykumar, M. Bhunia, S. K. Dey, S. K. Singh, S. Kurungot and S. K. Mandal, *J. Am. Chem. Soc*. ,2015, **137**, 5955–5960.
23. A. Mitra, A. Pariyar, S. Bose, P. Bandyopadhyay and A. Sarkar, *Sens. Actuators B,* 2015, **210**, 712–718.
24. A. Mitra, S. Bose, S. Biswas, P. Bandyopadhyay and A. Sarkar, *Chem Plus Chem,* 2018, **83**, 832–837.
25. P. Dutta, R. Sharma, S. Kumari, R. D. Dubey, S. Sarkar, J. Paulraj, G. Vijaykumar, M. Pandey, L. Sravanti, M. Samarla, H. S. Das, Yashpal, B Heeralal, R. Goyal, N. Gupta, S. K. Mandal, A. Sengupta and A. Sarkar, *Chem. Comm*, 2019, **55**, 1718-1721.
26. F. Carnovale, T. H. Gan, J. B. Peel and K. D. Franz, *JCS Perkin Trans II*., 1980, 957-960.
27. E. Gabano, E. Marengo, M. Bobba, E. Robotti, C. Cassino, M. Botta and D. Osella, *Coord. Chem. Rev*., 2006, **250**, 2158-2174.
28. Q. P. Qin , S.L. Wang, M.X. Tan, Z.F. Wang, X.L. Huang, Q.M. Wei, B.B. Shi, B.Q. Zou and H. Liang, *Metallomics*, 2018, **10**, 1160-1169.
29. L. Arzuman, P. Beale, Y. JQ and F. Huq, *Anticancer Research*,2016, **36**, 2809-2818.
30. G.Y. Park, J.J. Wilson, Y. Song and S.J. Lippard, *Proc Natl Acad Sci* USA ,2012, **109**, 11987-11992.
31. L. Arzuman, Y. JQ, F. Huq, P. Beale and N Proschogo, *Anticancer Res*, 2014, **34**, 7077-7090.
32. L. Arzuman, P. Beale, C. Chan, Y. JQ and F. Huq, *Anticancer Res*, 2014, **34**, 5453-5464.
33. G. H. W. Milburn and M. R. Truter, *J. Chem. Soc. A*, 1966, 1609-1616.

34. F. A. I. Al-Khodir, H. M. A. Abumelha, T. Al-Warhi, and S. A. Al-Iss, *Hindawi BioMed Research International*, **Volume 2019**, Article ID 9835745, https://doi.org/10.1155/2019/9835745.
35. A. K. Mishra, S. B. Mishra, N Manav, D. Saluja, R. Chandra and N. K. Kaushik, *Bioorganic & Medicinal* Chemistry, 2006, **14**, 6333–6340.
36. O. Rixe, W. Ortuzar, M. Alvarez, R. Parker, E. Reed, K. Paull and T. Fojo, *Biochem Pharmacol*, 1996 Dec 24, **52**,1855-65.
37. A. Vekris, D. Meynard, M.C. Haaz, M. Bayssas, J. Bonnet and J. Robert, *Cancer Res*, 2004, **64**, 356-62.
38. P Majumder, S.K. Pradhan, P.G. Devi, S. Pal and D. Dasgupta, *Subcell Biochem*. 2007, **41**, 145-89.
39. K. Jirsová and V. Mandys, *Mutat Res.* ,1994, **310**, 37-44.
40. C.A. Wallen, R. Higashikubo and J.L. Roti, *Cell Tissue Kinet.,* 1983 Jul, **16**, 357-65.
41. A. Ku¨ng, D. B. Strickmann, M. Galanski, B. K. Keppler, *Journal of Inorganic Biochemistry,* 2001, **86**, 691–698.
42. T. C. Johnstone, G. Y. Park, and S. J. Lippard, *Anticancer Res*., 2014, **34**, 471–476.
43. C. F. Koelsch and J.A. Anthes, *J. Org. Chem*.,1941, **6**, 558-565.
44. S.K. Mandal, M. E. Itkis, X. Chi, S. Samanta, D. Lidsky, R.W. Reed, R. T. Oakley, F. S. Tham and R. C. Haddon, *J. Am. Chem. Soc*., 2005, 127, **22**, 8185–8196.
45. K.D. Franz and R.L. Martin, *Tetrahedron*, 1978, **34**, 14, 2147-2151.
46. O.V. Dolomanov, L.J. Bourhis, R.J. Gildea, J.A.K. Howard and H. Puschmann, *J. Appl. Cryst*., 2009, **42**, 339-341.
47. L. Palatinus and G. Chapuis, *J. Appl. Cryst*.,2007, **40**, 786-790.
48. L. Palatinus and A.V.D. Lee, *J. Appl. Cryst*.,2008, **41**, 975-984.
49. L. Palatinus, S. J. Palatinus and S.V. Smaalen, *J. Appl. Cryst*., 2012, **45**, 575-580.
50. G.M. Sheldrick, *Acta Cryst*., 2015, **C71**, 3-8.
51. E. Lipiec, F.S. Ruggeri, C. Benadiba, A.M. Borkowska, J.D. Kobierski, J. Miszczyk, B.R. Wood, G.B. Deacon, A. Kulik, G. Dietler and W.M. Kwiatek, *Nucleic Acids Res*., 2019, **47**, e108.
52. J.M. Chacón and M.K. Gardner, *Cell Mol Bioeng*., 2013, **6**, 406-417.